Magnetoresistance of a double-layer hybrid system in a tilted magnetic field

Fariborz Parhizgar and Reza Asgari[*]

School of Physics, Institute for Research in Fundamental Sciences (IPM), Tehran 19395-5531, Iran
(Received 12 March 2014; revised manuscript received 10 July 2014; published 24 July 2014)

The magnetoresistance and Hall coefficient of a doped graphene layer are investigated in the presence of a tilted magnetic field. We consider a graphene layer assembled by either another graphene layer or by a two-dimensional electron gas (2DEG) layer and with the interlayer electron-electron interaction modeled within the random phase approximation. Our calculated magnetoresistances show different interlayer screening effects between decoupled graphene-graphene and graphene-2DEG systems. We also analyze the dependence of dielectric materials as well as the distance between the layers on magnetoresistances. The angle dependence of the Hall coefficient is studied and we show that a quite large Hall resistivity occurs in the graphene layer.

I. INTRODUCTION

Magnetoresistance [1], the change of a material's resistivity in the presence of an external magnetic field, has been of interest both as a tool to probe the fundamental properties of an electronic material and for technological applications. Classically, the magnetoresistance effect depends on both the strength of the magnetic field and the relative direction of the magnetic field with respect to the current due to the Lorentz force. For nonmagnetic metals, magnetoresistivity effects at low magnetic fields are very small, although the effect can become quite large for high magnetic fields.

The magnetoresistance of graphene, a one-atom-thick layer of carbon atoms arranged in a honeycomb lattice [2,3], in the presence of the in-plane magnetic field was studied by Hwang and Das Sarma by using the Boltzmann approach [4]. In the presence of an in-plane magnetic field, charge carriers of graphene are spin polarized and the effect of the magnetic vector potential is negligible owing to the one-atom thickness of graphene. The authors showed that the applied magnetic field gives rise to the increase of the resistivity of graphene up to a saturation field where all electrons of the conduction band are spin polarized. The magnetic field beyond the saturation field excites electrons from the valence band to the conduction band and leads to a negative differential magnetoresistance. In practice, it is difficult to reach the saturation magnetic field of a graphene layer, $B_S \sim 140\sqrt{\bar{n}}$, where $\bar{n}$ is in units of 10^{10} cm^{-2} and B_S is scaled by units of Tesla. Although using the low electron density of graphene is feasible in experiments [5], one has to use an extremely clean and pristine sample to meet the necessary condition in which impurity density is much less than the charge carrier density to avoid any localization regime.

The magnetoresistance properties of a graphene layer are in contrast to those obtained in conventional two-dimensional electron gas (2DEG) systems in which the resistivity increases up to a certain magnetic field and then saturates [6–9]. The magnetoresistance behavior of the 2DEG system can be understood by the Zeeman coupling and the reduction of screening of charge impurities in a polarized Fermi liquid system.

If the magnetic field has a small deviation from the sample plane, in addition to the spin polarization of conduction electrons, it gives rise to the Hall effect. Tilting the magnetic field has been shown to be a straightforward tool to disentangled spin and orbit effects in 2DEG systems [10]. The longitudinal resistivity and Hall coefficient of a conventional 2DEG have been investigated experimentally [11] and theoretically [9] in a slightly tilted magnetic field.

Assembling graphene, on the other hand, with various two-dimensional (2D) layers into artificial heterostructures to explore novel or tailed properties has been proposed [12] and realized in tunneling-effect transistors [13]. Hybridizing a gapless graphene layer with another gapless graphene layer makes the system a decoupled layer graphene (DLG) [14] where both layers are chiral and differs from a situation in which a gapless graphene is assembled by a 2DEG sample (G-2DEG) [15] which is a chiral-nonchiral hybrid system. This structure makes it possible to study transport properties of the graphene layer according to an interlayer electron-electron interaction.

In this paper, we consider a hybrid structure in the presence of a tilted magnetic field to explore the effect of the interlayer interaction on the magnetoresistance properties of the studied layer. The longitudinal resistivity and Hall coefficient of the studied graphene layer are explored and the results are compared with those results obtained for only a single-layer graphene in the presence of a magnetic field. We also analyze the dependence of the dielectric material which fills the space between the two layers as well as the distance between layers on the magnetoresistance and Hall coefficient and show that the interlayer interaction plays a vital role even at longer distances by using a strong dielectric material between the two layers. The angle dependence of the Hall coefficient is obtained and we show that a quite large Hall resistivity occurs in graphene for certain values of the carrier density and screened interaction. This particular result is in contrast to that obtained in a 2DEG system where the Hall coefficient increases up to 30%.

The paper is organized as follows: In Sec. II, we describe a model Hamiltonian of double-layer systems and then derive the conductivity and Hall coefficient of the studied layer in a tilted magnetic field. Section III is devoted to our numerical results of the longitudinal conductivity and Hall coefficient of the studied graphene layer in a hybrid structure. Finally, a brief summary of results is given in Sec. IV.
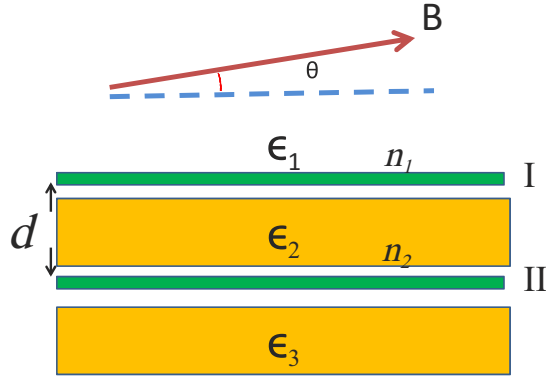
---

[*]asgari@ipm.ir

FIG. 1. (Color online) A schematic of a decoupled bilayer 2D system in the presence of a tilted magnetic field. In our study, the first layer is always graphene (studied graphene layer) with charge density n_1 and the second layer (layer II) is either a graphene layer or a 2DEG layer which is separated by a distance d from the studied graphene layer. The materials in the hybrid structure are indicated by their dielectric constants.

II. MODEL AND THEORY

We consider a double-layer structure incorporating a doped graphene layer (layer I) placed on another two-dimensional layer (layer II) with a separation distance d. A schematic of the structure is shown in Fig. 1, where layer II can be a chiral (another graphene) layer or a nonchiral (2DEG) layer. We assume each layer is of zero thickness in the direction normal to the plane of the system at zero temperature. The layers are separated by a dielectric material (shown in Fig. 1) with a dielectric constant ϵ_2 and we suppose that the tunneling of electrons between the layers is negligible; however, the Coulomb interlayer interaction plays a role in the system. The Hamiltonian of such a system can be written as [14]

$$\hat{H} = \hbar v_F \sum_{k,\gamma,\beta} \hat{\psi}_{k,\gamma}^\dagger (\sigma_{\gamma\beta} \cdot k) \hat{\psi}_{k,\beta} + \hat{T}_2$$

$$+ \frac{1}{2S} \sum_{q\neq 0, l, l'} V_{ll'}(q) \hat{\rho}_l(q) \hat{\rho}_{l'}(-q), \quad (1)$$

where γ, β are pseudospin indices in the x and y directions, $l = 1$ (2) is layer index, $v_F \simeq 10^6$ m/s is the Fermi velocity of graphene, and $\hat{\rho}_l(q)$ denotes the density operator in layer l with the momenta q. $\hat{T}_2$ denotes the kinetic energy of layer II, which is the same as the Dirac equation for a DLG system, while it is $\psi_{k,2}^\dagger \hbar^2 \hat{k}^2/(2m^*\psi_{k,2})$ in the case of a G-2DEG hybrid [15] where m^* is the electron band mass. The last term $V_{ll'}(q)$, refers to the inter- and intralayer electron-electron Coulomb interactions that can be obtained by using electrostatic relations for two parallel conducting systems [14]. The intralayer interaction is given by

$$V_{11}(q) = \frac{4\pi e^2}{q D(q)}[(\epsilon_2 + \epsilon_3)e^{qd} + (\epsilon_2 - \epsilon_3)e^{-qd}], \quad (2)$$

where

$$D(q) = [(\epsilon_1 + \epsilon_2)(\epsilon_2 + \epsilon_3)e^{qd} + (\epsilon_1 - \epsilon_2)(\epsilon_2 - \epsilon_3)e^{-qd}],$$

and the interlayer interaction is defined as

$$V_{12}(q) = V_{21}(q) = \frac{8\pi e^2}{q D(q)}\epsilon_2, \quad (3)$$

where ϵ_l denotes the dielectric constant of materials as illustrated in Fig. 1. Furthermore, the interaction in layer II can be obtained by replacing $\epsilon_1 \leftrightarrow \epsilon_3$ in $V_{11}(q)$. Notice that we are interested in the transport properties of layer I in the presence of layer II.

A. Conductivity and Hall coefficient in tilted magnetic field

Applying a tilted magnetic field with a small deviation from the layers' plane $\theta \ll 1$, where θ is the angle between the plane and the applied magnetic field, has two impacts. First of all, the parallel component of the magnetic field, $B_{||}$, gives rise to the spin polarization of carriers in the system and changes the chemical potential by $\pm\Delta/2$, where $\Delta = g^*\mu_B B_{||}$ with g^* being the effective Landé g factor and μ_B is the Bohr magneton. An enhanced g factor, $g^* = 2.7 \pm 0.2$, for single and bilayer graphene has been measured [16]. This enhancement is due to the impact of the electron-electron interaction in electronic liquid systems [17]. Notice that for $B_{||} = 0$, the spin degeneracy is $g_s = 2$ whereas for large $B_{||}$, the degeneracy factor is given by $g_s = 1$ and for the intermediate fields, the system is partially spin polarized. Furthermore, the electron density for spin up and spin down are given by

$$n^\pm = \frac{g_v}{4\pi\gamma^2}(\mu \pm \Delta/2)^2, \quad (4)$$

where μ is the chemical potential, g_v is the valley degeneracy, and γ is $\hbar v_F$. By increasing the magnetic field, the number of electrons with spin up increases and therefore the number of electrons with spin down decreases up to the saturation field B_{S1} in which $n^- = 0$. At this field $\mu = \Delta/2$, thus the saturation field is $B_{S1} = \sqrt{2}E_F/(g^*\mu_B)$ in which we use $n_1 = n^+ + n^- = E_F^2/(\pi\gamma^2)$ where E_F is the Fermi energy. Therefore, charge densities in term of the magnetic field can be changed and we thus have

$$n^\lambda = \begin{cases} \frac{n_1}{2}(\sqrt{1 - B'^2/2} + \lambda\sqrt{2}/(2B'))^2 & \text{if} \quad B' < 1 \\ n_1(\delta_{+,\lambda} + \frac{1}{4B'^2}(B'^2 - 1)^2) & \text{if} \quad B' > 1, \end{cases} \quad (5)$$

where $\lambda = \pm$, δ_{ij} is a Kronecker δ, and $B' = B_{||}/B_{S1}$. Accordingly, $B_{||}$ leads to a decomposition of the conductivity into two different spin-dependent channels; namely, σ_+ and σ_-, and the total conductivity is $\sigma = \sigma_+ + \sigma_-$ since the contributions of the spin-up and -down channels are parallel. Notice that in our study here, there is no mechanism to change spin direction.

It is worth mentioning that the magnetic field also affects the transport properties of layer II and leads to a change in the electron-density distribution. For a DLG system, the aforementioned formula remains the same for layer II with the electron density n_2, since generally, the two layers can have different electron densities. If we consider a 2DEG system as layer II, the magnetic field polarizes the spin of the conduction electron up to a saturation field which is $B_{S2} = 2\varepsilon_F/(g^*\mu_B)$, where ε_F is the Fermi energy of the 2DEG layer. Increasing the magnetic field cannot excite electrons from the valence band owing to the existence of a large band gap in the dispersion

relation of the 2DEG system. Therefore, the electron density in such a layer is

$$n^\lambda = \begin{cases} \frac{n_2}{2}(1 + \lambda B_{||}/B_{S2}) & \text{for} \quad B_{||} < B_{S2} \\ n_2 \delta_{+,\lambda} & \text{for} \quad B_{||} > B_{S2}. \end{cases} \quad (6)$$

The second consequence of the tilted magnetic field refers to the perpendicular component in which $B_\perp = B\sin(\theta)$. We assume that the field of strength is not strong enough to change the dispersion relation into the Landau levels producing the quantum Hall conductivity [18], and therefore it only results in an ordinary Hall conductivity σ_{xy}. Thus the electromagnetic fields, by using semiclassical relations [19], are given by

$$\mathbf{E} = \frac{1}{\sigma_+}(\mathbf{J}_+ + \beta_+ \mathbf{B} \times \mathbf{J}_+) = \frac{1}{\sigma_-}(\mathbf{J}_- + \beta_- \mathbf{B} \times \mathbf{J}_-), \quad (7)$$

where $\beta_i = e\tau_i v_F/(\hbar k_F^i c)$, $i = \pm$ indicates spin up or spin down, and k_F^i denotes the Fermi wave vector of the ith spin component with the electron density $n^\pm$. By using a current vector such as $\mathbf{J}_i = a_1^i \mathbf{E} + a_2^i \mathbf{B} \times \mathbf{E}$ and Eq. (7), it is easy to find a_1^i and a_2^i. We thus have $\mathbf{J} = a\mathbf{E} - b\mathbf{B} \times \mathbf{E}$ in which $\mathbf{J} = \mathbf{J}_+ + \mathbf{J}_-$ and

$$a = \sum_{i=+,-} \frac{\sigma_i}{1 + \beta_i^2 B_\perp^2}, \quad b = \sum_{i=+,-} \frac{\sigma_i \beta_i}{1 + \beta_i^2 B_\perp^2}. \quad (8)$$

Now, by considering the electric field, $\mathbf{E} = R_{xx}\mathbf{J} + R_H \mathbf{B} \times \mathbf{J}$, we calculate the magnetoresistance and Hall coefficient expressions as

$$R_{xx} = \frac{a}{a^2 + b^2 B_\perp^2}, \quad R_H = \frac{b}{a^2 + b^2 B_\perp^2}. \quad (9)$$

R_{xx} is the longitudinal resistivity and $R_H = R_{xy}/B_\perp$ is the Hall coefficient which depends on the conductivities of spin up and spin down which will be explored in the next section within the Boltzmann approximation.

Before describing the Boltzmann equation, it is worth mentioning that the conductivity of a two-component system can be written as

$$\sigma = \begin{pmatrix} \sigma_1 & \sigma_D \\ \sigma_D & \sigma_2 \end{pmatrix},$$

where σ_D is the drag conductivity. To calculate the resistivity, one should take the inverse of the conductivity matrix

$$\rho = \begin{pmatrix} \rho_1 & \rho_D \\ \rho_D & \rho_2 \end{pmatrix} = \frac{1}{\sigma_1 \sigma_2 - \sigma_D^2} \begin{pmatrix} \sigma_2 & -\sigma_D \\ -\sigma_D & \sigma_1 \end{pmatrix}. \quad (10)$$

Using the fact that $\sigma_D^2 \ll \sigma_1 \sigma_2$, the resistivity of each layer is obtained as $\rho_i = 1/\sigma_i$ and we therefore define the inverse of the conductivity as the resistivity in both longitudinal and Hall conductivities of layer I.

B. Boltzmann approach for conductivity

To calculate the conductivity of layer I in which the electron density n_1 is much larger than the concentration of impurities, n_{imp}, we therefore can use the Boltzmann approach which is based on the relaxation-time approximation. Our theory is formulated for weak disorder and we consider only charged impurity scattering without spin-flip processes. In this approach, the conductivity of the system is given by [20]

$$\sigma_\pm = \frac{e^2}{2} \hbar^2 v_F^2 \int d\varepsilon D^\pm(\varepsilon) \tau(\varepsilon) \left[-\frac{\partial n_F(\varepsilon)}{\partial \varepsilon} \right], \quad (11)$$

where $n_F(\varepsilon)$ is the Fermi distribution function. At zero temperature, the above equation reduces [4,20] to $\sigma_\pm = e^2 v_F^2 D(E_F^\pm) \tau(E_F^\pm)/2$, where $D(E_F^\pm)$ is the density of states at the Fermi energy and in the case of graphene $D(E_F^\pm) = g_s g_v E_F^\pm/(2\pi\gamma^2)$. $\tau(E_k)$ is the relaxation time which, for graphene layer, is given by [21]

$$\frac{1}{\tau(E_k)} = \frac{\pi}{\hbar} \sum_{k'} n_{\text{imp}} |W_{11}(q)|^2 [1 - \cos^2(\theta)] \delta(E_k - E_{k'}), \quad (12)$$

where $q = |k - k'|$, $\theta = \theta_k - \theta_{k'}$, and $W_{11}(q)$ represents the effective interaction between impurities and electrons. Short-range disorder plays a role in resistive scattering at higher carrier density and also high mobility [20]; however, for mid-range densities, the main scattering source is the charged-impurity disorder [22,23]. We thus neglect all disorder mechanisms other than random charged impurities in the system and assume the charged impurities to be of random negative sign of units of the electron charge. We assume that the charged disorder with density n_{imp} is located in the plane of layer I. Changing the variable $\sin(\theta/2) = y$ in Eq. (12) and writing the relation for different doping $n^\pm$ separately, the relaxation time reads

$$\frac{1}{\tau(E_F^\pm)} = \frac{4n_{\text{imp}}}{\pi\hbar} \frac{E_F^\pm}{\gamma^2} \int_0^1 dy |W_{11}(2k_F^\pm y)|^2 y^2 \sqrt{(1 - y^2)}, \quad (13)$$

where the relaxation time is evaluated at the $E_F^\pm$ of layer I with the electron density $n^\pm$ and the Fermi wave vector $k_F^\pm$. We use a minimal theory to describe effects of the parallel magnetic field. The effective interaction in the studied layer takes the form [14]

$$W_{11}(q) = \frac{V_{11}(q) + [V_{12}^2(q) - V_{11}(q)V_{22}(q)]\Pi_2^0(q)}{\varepsilon(q)}, \quad (14)$$

where the dielectric function $\varepsilon(q)$ within the random phase approximation (RPA) is

$$\varepsilon(q) = [1 - V_{11}(q)\Pi_1^0(q)][1 - V_{22}(q)\Pi_2^0(q)] - V_{12}^2(q)\Pi_1^0(q)\Pi_2^0(q), \quad (15)$$

where $\Pi_l^0(q)$ is the static charge response function of the lth layer and it is $D_F^+ P(q/k_F^+) + D_F^- P(q/k_F^-)$ for a doped graphene in the spin-polarized case, where

$$P(y) = -\begin{cases} 1 & \text{if} \quad y \leqslant 2 \\ 1 + \frac{\pi y}{8} - \frac{1}{2}\sqrt{1 - \frac{4}{y^2}} - \frac{y}{4}\sin^{-1}\left(\frac{2}{y}\right) & \text{if} \quad y > 2, \end{cases} \quad (16)$$

In the case that layer II is a 2DEG layer, we then need to modify the dielectric function by using $\Pi_2^0(q) = \Pi_2^+(q) + \Pi_2^-(q)$, where

$$\Pi_2^\pm(q) = D[1 - \sqrt{1 - (2k_{F2}^\pm/q)^2}\theta(q - 2k_{F2}^\pm)], \quad (17)$$

the density of states is $D = g_v m^*/(2\pi\hbar^2)$, and the Fermi wave vector is $k_{F2}^\pm = \sqrt{4\pi n_2^\pm/g_s}$.

By using Eq. (13), we can write the magnetoresistance of layer I in the presence of another layer as

$$\frac{\sigma}{\sigma^0} = \frac{1}{2}\left(\frac{I^0}{I^+} + \frac{I^0}{I^-}\right), \tag{18}$$

where

$$I^\pm = \frac{\sqrt{\pi(n_1+n_2)}}{2\pi e^2}\int_0^1 dy\, y^2\sqrt{1-y^2}\, W_{11}^2(2k_F^\pm y).$$

Notice that σ^0 and I^0 are the conductivity and I^+ of layer I when $B = 0$.

III. NUMERICAL RESULT AND DISCUSSION

In this section, we present our main numerical results based on the theory presented in the previous section. Our aim is to explore the impact of the correlation effects on the magnetoresistance and Hall coefficient of layer I. Layer II can be either a gapless graphene or a 2DEG layer. We therefore study the structures by considering both parallel and tilted magnetic fields. In all numerical results we use $e^2/\gamma = 2.2$ and $g^* = 2$.

A. Double-layer graphene in parallel magnetic field, $B_\perp = 0$

We consider a hybrid double-layer graphene system (DLG) in which the layers are coupled within the interlayer Coulomb interaction and they are separated by a dielectric material, as schematically illustrated in Fig. 1. We show the resistivity of layer I as a function of the $B = B_\parallel$ in Fig. 2 where electron densities are $n_1 = 10^{11}$ cm^{-2} and $n_2 = 10^{10}$ cm^{-2}, respectively. The resistivity is scaled by its value at zero magnetic field denoted by R_0 and it raises by increasing the magnetic field owing to the suppression of the screening and increases of the effective interaction screened within the RPA dielectric function. As B increases beyond its saturation-field value, $B_{S1} = \hbar v_F\sqrt{2\pi n_1}/(g^*\mu_B)$ in which layer I is fully spin polarized, the hole density is created in the valence band and makes R_{xx} decrease sharply, which demonstrates the negative differential magnetoresistance. We analyze the resistivity for the different layer distances d and the media dielectric constants ϵ_2, and our numerical results are shown in Figs. 2(a) and 2(b), respectively. Interestingly enough, Fig. 2(a) shows that the resistivity of layer I is significantly modified when $n_2 < n_1$. For $B > B_{S2}$, the effective interaction decreases, which gives rise to a decrease of the resistivity. Our numerical results show that the resistivity has a negative differential magnetoresistance for a small d value and for a region in which $B \ll B_{S1}$. This region depends on the electron density in layer II, n_2 and the slope of the R_{xx} changes by decreasing n_2 at small B. Thus, a larger conductivity of layer I can be reached by using $n_2 < n_1$. It is obvious that we also get the resistivity of a single graphene layer by considering a very large d value.

Moreover, it has been shown that [24] the dielectric constant between the two layers in double-layer graphene systems has a significant role in transport properties. Although increasing
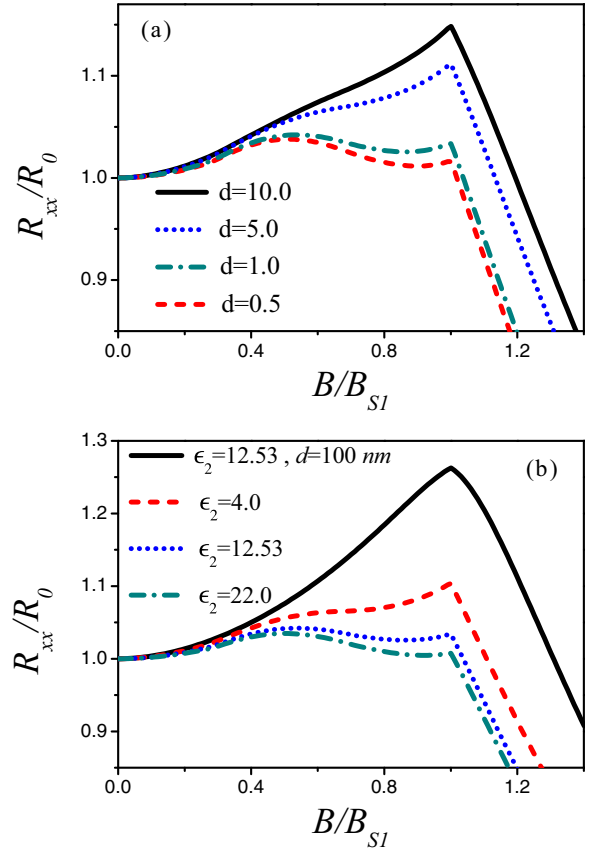

FIG. 2. (Color online) Longitudinal resistivity of layer I in a hybrid double-layer system composed by the doped graphene sheet that is Coulomb coupled to another doped graphene in which they are separated by a dielectric material as a function of $B = B_\parallel$ for (a) different distance between layers in units of nm for $\epsilon_2 = 12.53$ and (b) different value of ϵ_2 with constant distance $d = 1.0$ nm. We also consider a plot with $d = 100$ nm to suppress the interlayer effect. We choose $\epsilon_1 = 1.0, \epsilon_3 = 12.53$, and the electron densities are $n_1 = 10^{11}$ cm^{-2} and $n_2 = 10^{10}$ cm^{-2}, respectively.

the dielectric constant screens the interlayer interaction, it has a significant role on the intralayer screening of the considered layer, too. Accordingly, a competition between the effect of the inter- and intralayer interactions on the magnetoresistance of layer I is vital when dielectric materials with higher ϵ_2 are used. We also obtain the reduction of the resistivity when the dielectric constant increases. We choose three different materials, namely h-BN, Al$_2$O$_3$, and HfO$_2$ for $d = 1$ nm to explore the effect of the interlayer interaction on the magnetoresistance of layer I in the DLG system. In the same manner, we obtain the negative differential magnetoresistance in area which $B < B_{S1}$ due to the correlation effects induced in layer I from layer II.

We analyze the resistivity at the saturation magnetic field for layer I as a function of d in Fig. 3. We obtain a resistivity enhanced by about 20% by increasing the layer distance for the case in which there is a larger dielectric constant between layers owing to the long-range interlayer interaction and the fact that $V_{12}(q)$ is proportional to ϵ_2. $R_{xx}(B_{S1})$ significantly changes for a small d and ϵ_2.
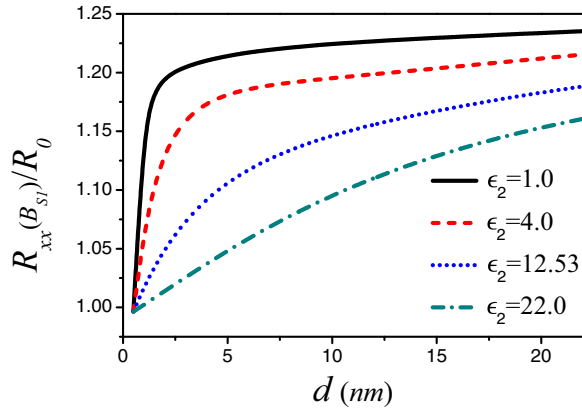
FIG. 3. (Color online) Longitudinal resistivity of layer I at the saturation field versus the distance between layers in units of nm in a hybrid double-layer graphene system for different values of ϵ_2. We choose $\epsilon_1 = 1.0$, $\epsilon_3 = 12.53$, and the electron densities are $n_1 = 10^{11}$ cm^{-2} and $n_2 = 10^{10}$ cm^{-2}, respectively.

B. Graphene-2DEG hybrid in parallel magnetic field, $B_\perp = 0$

In this section, we consider a G-2DEG system in which a dielectric material is filled in the space between the two layers. For such a system, the saturation magnetic field of the 2DEG layer, $B_{S2} = 2\pi\hbar^2 n_2/(g_v m^* g^* \mu_B)$ is smaller than the corresponding one in a graphene-layer system, B_{S1}, even though $n_1 = n_2$.

Figure 4 shows the longitudinal magnetoresistance of layer I in the presence of the 2DEG layer for different materials [25]. The electron density of both layers is the same and equal to 10^{11} cm^{-2}, $\epsilon_1 = 1$, and $\epsilon_2 = \epsilon_3$ for $d = 10$ nm. This figure shows that, because 2DEG carriers are fully polarized, the magnetoresistance of layer I exhibits a sharp jump at B_{S2},
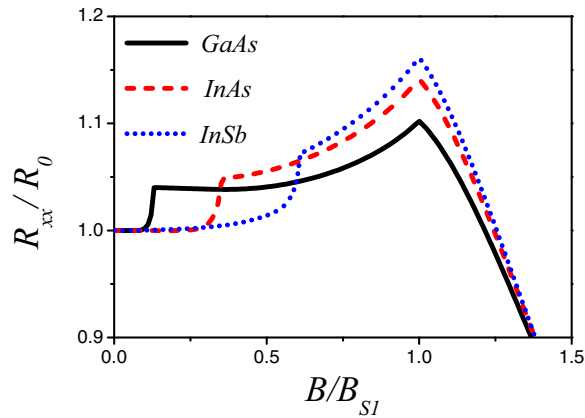

FIG. 4. (Color online) Magnetoresistance of layer I as a function of the $B = B_{||}$ in the presence of a 2DEG layer for different 2DEG materials. Here, the dielectric constants of 2DEG systems are chosen as [25] 10.9, 12.2, and 15.7; in addition, the effective mass of these materials are the electron-band effective mass which is $0.07m$, $0.026m$, and $0.015m$ where m is the electron bare mass for GaAs, InAs, and InSb, respectively. The electron density of the both layers is the same and equal to 10^{11} cm^{-2}, $\epsilon_1 = 1$, $\epsilon_2 = \epsilon_3$, which are equal to the dielectric constant of the 2DEG layer and the distance between layers is $d = 10$ nm.
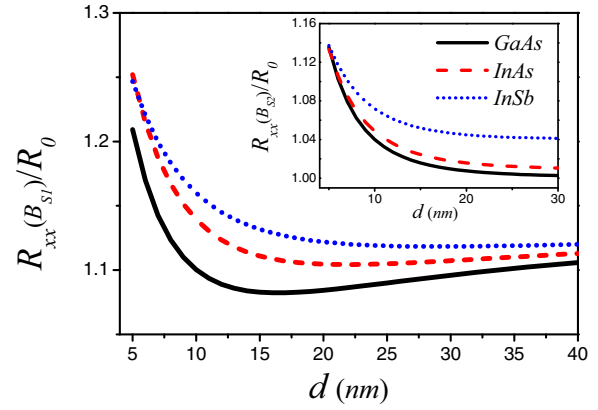

FIG. 5. (Color online) Value of the saturation field resistivity of layer I scaled by its zero-field resistivity as a function of d in the presence of different 2DEG materials. Inset is the same for the saturation field of layer II. All other parameters are the same as Fig. 4.

which occurs at a much smaller value than the B_{S1} value. The longitudinal resistivity increases by increasing ϵ_2 due to the increased screening. Importantly, this feature differs from that in a DLG structure. Meanwhile, since $B_{S2} \sim m^{*-1}$, the position of the first peak of the R_{xx} decreases by increasing the electron effective mass.

In order to bring out the difference between G-2DEG and DLG systems, we plot the magnetoresistance of layer I at the saturation magnetic field B_{S1} in Fig. 5 when the 2DEG layer is placed near the graphene layer. The results show that the R_{xx} decreases at small d, behaves nonmonotonically as a function of d, and the results are in a different trend as compared with Fig. 3 in which the results for DLG systems are shown. The difference can be understood in terms of the effect of the chirality effect in the charge-charge response function of the doped graphene [26].

C. Longitudinal resistivity in tilted magnetic field, $B = (B_{||}^2 + B_\perp^2)^{1/2}$

In the presence of a tilted magnetic field $B = (B_{||}^2 + B_\perp^2)^{1/2}$ where $B_{||} \gg B_\perp$, we should use the full expression of the conductivity given in Eq. (9) and it can be written as

$$B_\perp \beta_\pm = \frac{B I_0 n_t}{2 B_{S1} I^\pm n_1^\pm} x = \alpha_\pm x, \qquad (19)$$

where $I^\pm$ is the function given under Eq. (18), and n_t is the total density of the two layers ($n_1 + n_2$). Here, we define a new parameter [9], $x = 0.895 \sin(\theta)\sqrt{\bar{n}_1}/(\bar{n}_{\rm imp} I_0)$ ($\bar{n}_1$ and $\bar{n}_{\rm imp}$ are in units of 10^{12} cm^{-2}). Note that x depends on both the angle as well as $n_{\rm imp}$, therefore larger values of x can be obtained by using clean samples.

In order to understand the impact of the tilted magnetic field on the resistivity, we first examine R_{xx} of an isolated graphene sheet in the presence of B. Figure 6(a) shows the effect of the tilted magnetic field on the longitudinal resistivity of an isolated n-doped graphene sheet. The longitudinal resistivity increases by increasing the value of x. The magnitude of differential magnetoresistance changes significantly in
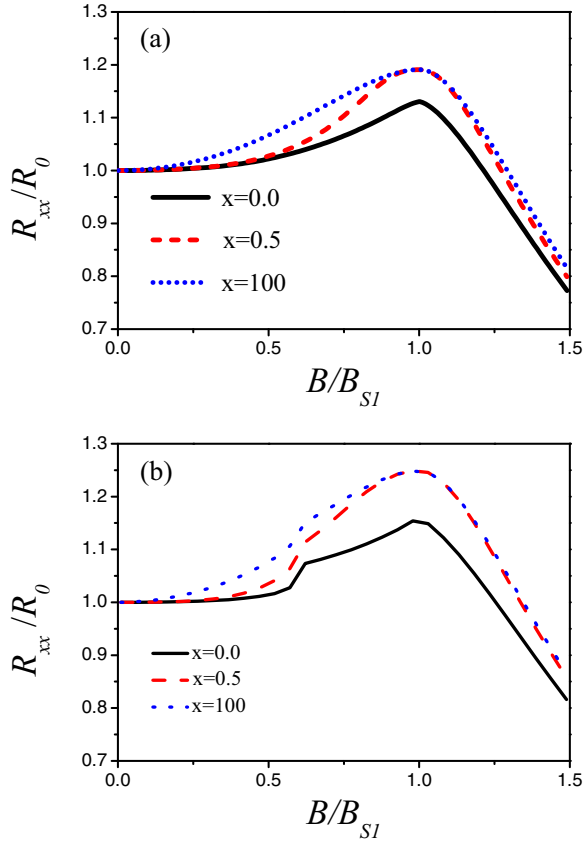
FIG. 6. (Color online) Longitudinal magnetoresistivity of a system consisting of (a) a single graphene layer ($\epsilon_2 = 12.52$, $\epsilon_1 = 1.0$) with $n_1 = 10^{12}$ cm^{-2} and (b) in a hybrid system in which a G-2DEG system for InSb with $n_1 = n_2 = 0.1 \times 10^{12}$ cm^{-2}, $\epsilon_3 = 15.7$, and $d = 10$ nm as a function of the magnetic-field amplitude $B = (B_{||}^2 + B_{\perp}^2)^{1/2}$. The magnetoresistance is calculated for different values of the tilting parameter x.

D. Hall resistivity in tilted magnetic field

Finally, by applying the tilted magnetic field, $B = (B_{||}^2 + B_{\perp}^2)^{1/2}$ in which there is a weak perpendicular component $B_{\perp}$ and using two-species conductivities σ_+ and σ_-, we can straightforwardly calculate the Hall coefficient $R_H = R_{xy}/B_{\perp}$ from Eq. (9). Normalizing the Hall coefficient to its zero-magnetic-field value, $R_{H0} = R_H(B \to 0)$ one gets

$$R_H/R_{H0} = \frac{b}{a^2 + b^2 B_{\perp}^2} \frac{\sigma_0}{\beta_0}. \qquad (20)$$

Note that $\beta_+ = \beta_-$ for the limit of $B_{||} \to 0$ and $\beta_0 = \beta_+(B = 0)$. The Hall coefficient of a 2DEG system shows a peak before the saturation-magnetic-field point and reaches a constant value at the saturation magnetic field [9]. Moreover, the Hall coefficient of the 2DEG system increases monotonically by decreasing the x value; however, our numerical results show that the Hall coefficient of layer I is significantly enhanced by decreasing the x values.

In Fig. 7, the behavior of the Hall coefficient of layer I as a function of the $B = (B_{||}^2 + B_{\perp}^2)^{1/2}$ is shown in the presence of the InAs 2DEG for different values of x. Same qualitative results can be obtained for a single graphene layer and therefore we conclude that the Hall coefficient of graphene differs from that result of the 2DEG system. As is obvious in this figure, the two peaks occur at finite x. Importantly, if we interpret the Hall resistivity as an effective density of charge carriers, our numerical results show that the effective density of carriers changes more sharply around the B_{S1}. Nevertheless, the Hall coefficient in layer I has two peaks at finite x values in which one peak occurs just below the B_{S1} value and another takes place above that. These peaks become sharper at smaller x; accordingly, a giant-like Hall coefficient behavior of layer I can be reached at a small value of x. Notice that at $B \simeq B_{S1}$ the Hall coefficient decreases and eventually reaches to R_{H0} at $B = B_{S1}$. To understand these features, we analytically
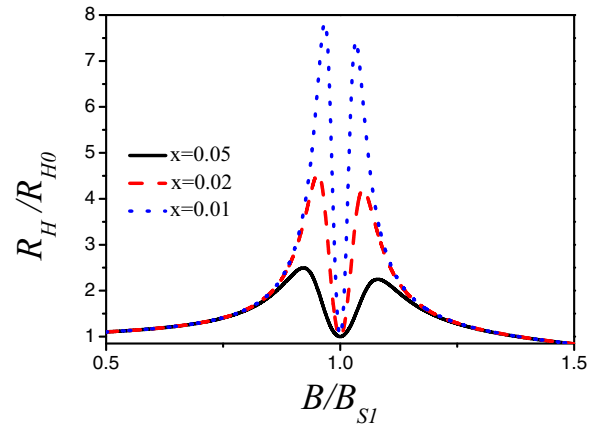
comparison with that result obtained when $B_{\perp} = 0$. Moreover, the maximum of the R_{xx} at the B_{S1} is not sensitive to the finite value of x and shows good agreement with those trends obtained in experiment [16,27]. It should be noted that the maximum of the R_{xx} is a good quantity to explore quantum states in a graphene system and for this purpose, the magnetoresistance of the insulating state that forms at the charge neutrality point in the presence of tilted magnetic field has been measured [28] and data indicated that the zero-filling factor quantum Hall state in single layer graphene is not spin polarized. We choose $x = 100$ for an extremely clean sample and this figure shows that the R_{xx} increases slightly by increasing large value of x. Having known the behavior of R_{xx} as a function of B for a single graphene sheet, we could explore R_{xx} for layer I in a hybrid system. We consider only a G-2DEG system for an InSb layer with $n_1 = n_2 = 0.1 \times 10^{12}$ cm^{-2}, $\epsilon_3 = 15.7$, and $d = 10$ nm, and R_{xx} is shown as a function of B in Fig. 6(b). As it is seen, R_{xx} increases with increasing x value and the fact that $B_{S2} < B_{S1}$, a sharp change in the results at B_{S2} still remains. These numerical results exhibit that the interlayer interaction has a more significant effect, especially for a small value of x.

FIG. 7. (Color online) Hall coefficient of layer I as a function of the magnetic field amplitude, $B = (B_{||}^2 + B_{\perp}^2)^{1/2}$ in the presence of the 2DEG InAs for different values of x at given constant $\theta = 4°$. We consider $\epsilon_3 = \epsilon_2 = 12.2$, $m^* = 0.026 m_e$, and $n_1 = 0.1 \times 10^{12}$ cm^{-2}, $n_2 = 0.01 \times 10^{12}$ cm^{-2}. The layers are separated with a distance $d = 10$ nm.

calculate the R_H in different regions. Let us start off by using the definition of the Hall coefficient of layer I:

$$
\frac{R_H}{R_{H0}} = \frac{\sigma_0}{\beta_0} \frac{b}{a^2 + b^2 B_\perp^2}
$$

$$
= \frac{D\sigma_0}{\beta_0} \frac{\sigma_+\beta_+(1+x^2\alpha_-^2) + \sigma_-\beta_-(1+x^2\alpha_+^2)}{[\sigma_+(1+x^2\alpha_-^2) + \sigma_-(1+x^2\alpha_+^2)]^2 + x^2[\sigma_+\alpha_+(1+x^2\alpha_-^2) + \sigma_-\alpha_-(1+x^2\alpha_+^2)]^2}, \tag{21}
$$

where $D = (1 + x^2\alpha_+^2)(1 + x^2\alpha_-^2)$. Notice that, in the above equation, there is a competition between x and α_- since α_- is proportional to $1/n^-$ and diverges at $B = B_{S1}$ where $n^- = 0$, thus the zero limit of x cannot prevent this singular behavior. We take the limit $x\alpha_- \to 0$ around B_{S1}. Notice that σ_- has a finite nonzero value even at $B = B_{S1}$ [20].

By considering a case that $x \to 0$ and $\alpha_- \to \infty$, however, $x\alpha_- \to 0$ in which the Hall resistivity is noticeably large, we have

$$
\frac{R_H}{R_{H0}} = \frac{D\sigma_0}{\beta_0} \frac{\sigma_+\beta_+ + \sigma_-\beta_-}{(\sigma_+ + \sigma_-)^2 + x^2(\sigma_+\alpha_+ + \sigma_-\alpha_-)^2}
$$

$$
= \frac{n_1 I_0^2}{4n_\pm I_\pm^2}, \tag{22}
$$

which has a large value at B close to the B_{S1} in which n^- becomes very small. It should be noted that such a huge resistivity does not appear in a 2DEG since the Hall coefficient of a 2DEG at $x = 0$ is given by [9]

$$
R_H/R_{H0} = \frac{2\sum_\pm n_\pm(I_0/I_\pm)^2}{\left(\sum_\pm n_\pm I_0/I_\pm\right)^2}, \tag{23}
$$

which is a constant at $x \to 0$. On the other hand, if we consider the case $\alpha_- \to \infty$ and $x\alpha_- \to \infty$ as well, the R_H will be independent of the x value, too. In this limit, Eq. (21) takes the following form:

$$
\frac{R_H}{R_{H0}} = \frac{D\sigma_0}{\beta_0} \frac{\sigma_+\beta_+(x^2\alpha_-^2) + \sigma_-\beta_-(1+x^2\alpha_+^2)}{[\sigma_+(x^2\alpha_-^2)]^2 + x^2[\sigma_+\alpha_+(x^2\alpha_-^2)]^2}. \tag{24}
$$

By using the approximation $\beta_- \sim \alpha_-$ in this limit, the term with α_-^2 dominates and also $D \to (1 + x^2\alpha_+^2)x^2\alpha_-^2$, and thus we get

$$
\frac{R_H}{R_{H0}} = \frac{\sigma_0\beta_+}{\sigma_+\beta_0} = \frac{n_1}{n^+}. \tag{25}
$$

Interestingly, this ratio becomes unity when $B = B_{S1}$. Figure 8 shows the behavior of the normalized R_H/R_{H0} as a function of the magnetic field for different values of x for different systems. As shown, the Hall coefficients have a peak in region $B < B_{S1}$ which is the same as one gets in a 2DEG system; however, it changes for $B > B_{S1}$ and the results depend on the value of x. The peak at $B > B_{S1}$ becomes larger by reducing n_2 and increases the interlayer correlation. By increasing x value, the shape of the Hall coefficient changes significantly and decreases rapidly as x increases. Contrary to the R_{xx} where the interaction with graphene (2DEG) makes lower (higher) values of the magnetoresistance of layer I, the interlayer interaction always makes R_H/R_{H0} increase compared to its single-layer values.

IV. CONCLUSION

In summary, we calculated the longitudinal resistivity and Hall coefficient of the gapless graphene (layer I) in a hybrid structure and compared the results with those of a single layer of graphene in the presence of a tilted magnetic field. We assumed that the magnetic field is slightly off the electronic planes so that there is a weak perpendicular component.

For a parallel magnetic field, $B_\perp = 0$, we analyzed the dependence of the dielectric material which fills the space between the two layers as well as the distance between the layers on the magnetoresistances of layer I and showed that the interlayer interaction plays an important role even at longer distances by using large values of the dielectric constant. Our numerical results show that the resistivity of layer I is significantly modified when $n_2 < n_1$. Moreover, the resistivity
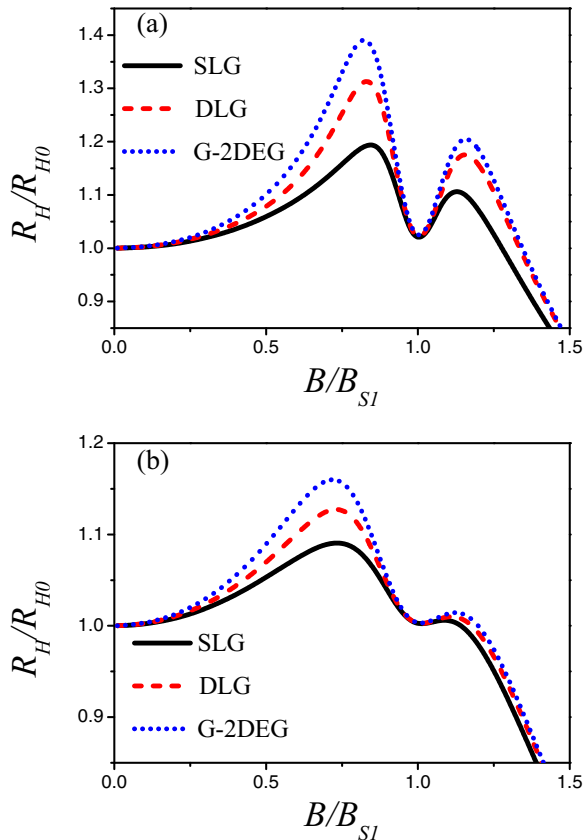
FIG. 8. (Color online) Hall coefficient of a single layer graphene (SLG) and Hall coefficient of layer I in a DLG and G-2DEG systems as a function of the magnetic-field amplitude, $B = (B_\parallel^2 + B_\perp^2)^{1/2}$ at given constant $\theta = 4°$ for (a) $x = 0.2$ and (b) $x = 0.5$. The electron densities are $n_1 = 0.1 \times 10^{12}$ cm^{-2} and $n_2 = 0.01 \times 10^{12}$ cm^{-2}, respectively, and the layers are separated by a distance $d = 10$ nm.

shows a negative differential magnetoresistance for a small d and for a region in which $B_{||}$ is much smaller than the saturation magnetic field. We also obtained the reduction of the resistivity when the dielectric constant between two layers increases and obtained the negative differential magnetoresistance in the area where $B_{||} < B_{S1}$ due to the correlation effects induced on layer I from another layer. We showed that R_{xx} in a G-2DEG structure decreases at small d, behaves nonmonotonically as a function of d, and the results show in different trend as compared to those in DLG systems.

In the presence of a tilted magnetic field B, the Hall coefficient of layer I shows two peaks at finite x values in which one peak occurs just below the B_{S1} value and another takes place above that. These peaks become sharper at very small x values. Accordingly, a giant-like Hall coefficient behavior for layer I can be reached in a hybrid graphene structure. We have shown that the magnetoresistance and the Hall coefficient of a doped graphene layer can be tuned by the electron density and dielectric constants of the materials in a hybrid structure. Our results should be verified by experiments.

[1] E. L. Nagaev, Phys. Rep. **346**, 387 (2001).

[2] K. S. Novoselov, A. K. Geim, S. V. Morozov, D. Jiang, Y. Zhang, S. V. Dubonos, I. V. Grigorieva, and A. A. Firsov, Science **306**, 666 (2004).

[3] A. H. Castro Neto, F. Guinea, N. M. R. Peres, K. S. Novoselov, and A. K. Geim, Rev. Mod. Phys. **81**, 109 (2009).

[4] E. H. Hwang and S. Das Sarma, Phys. Rev. B **80**, 075417 (2009).

[5] L. A. Ponomarenko, A. K. Geim, A. A. Zhukov, R. Jalil, S. V. Morozov, K. S. Novoselov, V. V. Cheianov, V. I. Fal'ko, K. Watanabe, T. Taniguchi, and R. V. Gorbachev, Nat. Phys. **7**, 958 (2011).

[6] A. A. Shashkin, S. V. Kravchenko, V. T. Dolgopolov, and T. M. Klapwijk, Phys. Rev. Lett. **87**, 086801 (2001); T. Okamoto, K. Hosoya, S. Kawaji, and A. Yagi, *ibid.* **82**, 3875 (1999); S. A. Vitkalov, H. Zheng, K. M. Mertes, M. P. Sarachik, and T. M. Klapwijk, *ibid.* **87**, 086401 (2001).

[7] D. Simonian, S. V. Kravchenko, M. P. Sarachik, and V. M. Pudalov, Phys. Rev. Lett. **79**, 2304 (1997); Phys. Rev. B **57**, R9420(R) (1998); M. Y. Simmons, A. R. Hamilton, M. Pepper, E. H. Linfield, P. D. Rose, D. A. Ritchie, A. K. Savchenko, and T. G. Griffiths, Phys. Rev. Lett. **80**, 1292 (1998); J. Yoon, C. C. Li, D. Shahar, D. C. Tsui, and M. Shayegan, *ibid.* **82**, 1744 (1999).

[8] S. Das Sarma and E. H. Hwang, Phys. Rev. B **72**, 205303 (2005); V. T. Dolgopolov and A. Gold, JETP Lett. **71**, 27 (2000).

[9] Igor F. Herbut, Phys. Rev. B **63**, 113102 (2001).

[10] A. Yu. Kuntsevich, L. A. Morgun, and V. M. Pudalov, Phys. Rev. B **87**, 205406 (2013).

[11] S. A. Vitkalov, H. Zheng, K. M. Mertes, M. P. Sarachik, and T. M. Klapwijk, Phys. Rev. B **63**, 193304 (2001).

[12] K. S. Novesolov and A. H. Castro Neto, Phys. Scr. **146**, 014006 (2012).

[13] J. W. Yu *et al.*, Nat. Mater. **12**, 246 (2013); L. Britnel *et al.*, Science **335**, 947 (2012); C. Dean *et al.*, Solid State Commun. **152**, 1275 (2012).

[14] R. E. V. Profumo, M. Polini, R. Asgari, R. Fazio, and A. H. MacDonald, Phys. Rev. B **82**, 085443 (2010).

[15] Alessandro Principi, Matteo Carrega, Reza Asgari, Vittorio Pellegrini, and Marco Polini, Phys. Rev. B **86**, 085421 (2012).

[16] E. V. Kurganova, H. J. van Elferen, A. McCollam, L. A. Ponomarenko, K. S. Novoselov, A. Veligura, B. J. van Wees, J. C. Maan, and U. Zeitler, Phys. Rev. B **84**, 121407 (2011).

[17] R. Asgari and B. Tanatar, Phys. Rev. B **74**, 075301 (2006).

[18] Takao Morinari and Takami Tohyama, Phys. Rev. B **82**, 165117 (2010); J. Jobst, D. Waldmann, I. V. Gornyi, A. D. Mirlin, and H. B. Weber, Phys. Rev. Lett. **108**, 106601 (2012).

[19] J. M. Ziman, *Principles of the Theory of Solids* (Cambridge University Press, Cambridge, 1972).

[20] S. Das Sarma, Shaffique Adam, E. H. Hwang, and Enrico Rossi, Rev. Mod. Phys. **83**, 407 (2011).

[21] E. H. Hwang and S. Das Sarma, Phys. Rev. B **77**, 195412 (2008).

[22] T. Ando, J. Phys. Soc. Jpn. **75**, 074716 (2006); V. V. Cheianov and V. I. Fal'ko, Phys. Rev. Lett. **97**, 226801 (2006); K. Nomura and A. H. MacDonald, *ibid.* **98**, 076602 (2007); E. H. Hwang, S. Adam, and S. Das Sarma, *ibid.* **98**, 186806 (2007).

[23] P. S. Alekseev, A. P. Dmitriev, I. V. Gornyi, and V. Yu. Kachorovskii, Phys. Rev. B **87**, 165432 (2013).

[24] Kazuhiro Hosono and Katsunori Wakabayashi, Appl. Phys. Lett. **103**, 033102 (2013).

[25] Neil. W. Ashcroft and N. David Mermin, *Solid State Physics* (Harcourt College Publishers, Cambridge, 1976).

[26] Y. Barlas, T. Pereg-Barnea, M. Polini, R. Asgari, and A. H. MacDonald, Phys. Rev. Lett. **98**, 236601 (2007).

[27] Wei Han, W. H. Wang, K. Pi, K. M. McCreary, W. Bao, Yan Li, F. Miao, C. N. Lau, and R. K. Kawakami, Phys. Rev. Lett. **102**, 137205 (2009).

[28] Yue Zhao, Paul Cadden-Zimansky, Fereshte Ghahari, and Philip Kim, Phys. Rev. Lett. **108**, 106804 (2012).